ISSN 0023-1584, Kinetics and Catalysis, 2016, Vol. 57, No. 1, pp. 95–103. © Pleiades Publishing, Ltd., 2016.
Original Russian Text © D.E. Zavelev, A.V. Chistyakov, G.M. Zhidomirov, M.A. Gubanov, M.V. Tsodikov, I.I. Moiseev, 2016, published in Kinetika i Kataliz, 2016, Vol. 57, No. 1, pp. 97–105.

Mechanism of the Reductive Dehydration of Ethanol into C_{3+} Alkanes over the Commercial Alumina–Platinum Catalyst AP-64

D. E. Zavelev[a], *, A. V. Chistyakov[a], G. M. Zhidomirov[b, c], M. A. Gubanov[a], M. V. Tsodikov[a], and I. I. Moiseev[a, d]

[a] *Topchiev Institute of Petrochemical Synthesis, Russian Academy of Sciences, Moscow, 119991 Russia*
[b] *Boreskov Institute of Catalysis, Siberian Branch, Russian Academy of Sciences, Novosibirsk, 630090 Russia*
[c] *Zelinsky Institute of Organic Chemistry, Russian Academy of Sciences, Moscow, 119991 Russia*
[d] *Gubkin State University of Oil and Gas, Moscow, 119991 Russia*
**e-mail: metalian@ips.ac.ru*

Received July 7, 2015

Abstract—The mechanism of the reductive dehydration of ethanol (RDE) into C_{3+} alkanes over the commercial alumina–platinum catalyst AP-64 has been investigated. The catalyst pre-reduction time has an effect on the conversion of ethanol and on that of ethylene, a possible intermediate compound in the RDE reaction. Over the catalyst reduced for 12 h, ethanol turns into a C_3–C_{12} alkane fraction and ethylene turns into a C_3–C_{12} olefin fraction, whose yields are 39.0 and 31.4%, respectively. Energetic parameters of ethanol chemisorption and conversion on a Pt_6Al_4 cluster have been determined by the density functional theory method using the PRIRODA 13 program. Ethanol dehydration into ethylene proceeds via the successive breaking of C–H and C–O bonds, and the rate-determining step of the process depends on the atom (Pt or Al) to which the OH group of the alcohol is coordinated. Hydroxyl group transfer from the Pt atom to the nearest Al atom is energetically favorable here. It is hypothesized that the main role of the metal-containing cluster is donation of chemisorbed ethylene to the nearest acid sites, on which the ethylene oligomerizes into a C_3–C_{10} hydrocarbon fraction.

Keywords: reductive dehydration of ethanol, alumina–platinum catalysts, density functional theory

DOI: 10.1134/S0023158416010134

In the last decade, great attention in catalysis has been focused on developing approaches to the problem of efficiently converting biomass and its main products into energy carriers and valuable monomers [1–3]. The most important present-day energy carriers include purified hydrocarbon components of motor fuels, hydrogen, and synthesis gas. It was found that, after being appropriately modified or pre-activated, some common industrial catalysts show high selectivity in the conversion of ethanol, fermentation products, rapeseed oil, and cellulose into hydrocarbon components [4–7]. For example, the common commercial catalyst AP-64 changes its selectivity in ethanol and rapeseed oil conversion on being subjected to prolonged reductive activation followed by treatment with steam [7]. After a conventional, short-term, 2- to 4-h-long, reductive activation of the catalyst, ethanol turns into well-known organic products, such as ethylene, diethyl ether (small amounts), and CO; by contrast, upon the reductive activation of the catalyst for 12 h or a longer time at 450°C, ethanol (in argon) turns at 300–350°C into a C_3–C_{10+} alkane fraction dominated by linear-chain alkanes with an even number of carbon atoms, the yield of this fraction being up to 40% [8]. Below 300°C, the main ethanol conversion product is diethyl ether. There have been experiments on ethanol dehydration in the presence of a mechanical mixture of AP-64 and the hydrided intermetallide $Fe_{0.45}Ti_{0.5}Mo_{0.02}Zr_{0.03}H_x$ with various hydrogen contents, which was employed as a hydrogen donor, and it was demonstrated that, as the amount of hydrogen donated into the reaction zone is increased, the alumina–platinum catalyst loses its hydrocarbon fraction formation selectivity and the ethane yield increases [8]. The addition of hypothetical intermediate products of the reaction to ethanol demonstrated that a noticeable increase in the hydrocarbon fraction yield is observed upon the addition of ethylene and diethyl ether [4, 9, 10]. Note that diethyl ether under the same conditions turns into an alkane fraction that is similar in hydrocarbon composition to the fraction obtained from ethanol [11]. The addition of acetaldehyde does not increase the alkane yield. Still earlier [12], it was established that diethyl ether is among the intermediate products in ethanol conversion into tetrahydrofuran over Pt/C. These results suggest the following general scheme for ethanol conversion [13]:

$$\begin{tikzcd}
 & C_2H_{4ads} \arrow[r, "\text{Pt active site}"] & C_nH_{2n} \arrow[r, "Pt", "2[H]"'] & C_nH_{2n+2}. \\
n[C_2H_5OH]_s \arrow[ur] \arrow[dr, shift left] & & & \\
 & (C_2H_5)_2O \arrow[ul, shift left] \arrow[uu] & &
\end{tikzcd}$$

XAFS studies of the catalyst structure and morphology demonstrated that, upon prolonged reductive activation of the catalyst followed by steam treatment, the Pt atoms interact with Al atoms to the point of the formation of 0.257-nm-long Pt–Al bonds, which are characteristic of the Pt_2Al intermetallide [11, 14]. It was found by temperature-programmed ammonia desorption that the prolonged reduction and subsequent treatment of the catalyst with steam radically change the nature of the active sites of the γ-alumina support: the desorption peaks of the most common probe molecules shift to 600–650°C [11], indicating the conversion of aprotic acid sites into strong Brønsted acid sites that are as strong as the sites of zeolite catalysts [15]. These earlier results stimulated us to carry out a theoretical study of the most likely steps of ethanol conversion into an alkane fraction, which is referred to as reductive dehydration.

Here, we report the effect of the degree of reduction of the platinum-containing component of an alumina–platinum catalyst on its selectivity in direct ethanol conversion into alkanes and in the oligomerization of ethylene (which is an intermediate product in the reductive dehydration of ethanol into the C_{3+} hydrocarbon fraction). We have also carried out a theoretical analysis of one of the possible pathways of ethanol conversion on platinum–aluminum clusters of the reduced catalyst.

EXPERIMENTAL

We examined the commercial alumina–platinum catalyst AP-64 (~0.6 wt % Pt supported on γ-Al_2O_3, $S_{BET} \approx 200$ m^2/g, $V_{pore} = 0.65$ cm^3/g) produced by the Novokuibyshevsk Catalysts Plant, Russia.

The catalytic activity of AP-64 in the conversion of ethylene and ethylene-containing ethanol was studied in a reactor with a fixed catalyst bed using a laboratory flow circulation setup ensuring continuous recycling of the reaction gases. A detailed description of the setup is presented in an earlier publication [4]. Ethanol was delivered using a Gilson 307 high-precision doser (Gilson, United States) at an hourly space velocity of 0.6 h^{-1} and an argon pressure of 5 atm. The gas circulation rate was 50 cm^3/min. Ethylene conversion was performed in the circulation mode in an argon medium at a total pressure of 50 atm (ethylene partial pressure of 45 atm) and a temperature of 350°C for 2 h.

The gaseous products of the reaction were analyzed online by gas chromatography (GC), Gaseous C_1–C_5 hydrocarbons were analyzed on a Kristall 4000M chromatograph (Khromatek, Russia) fitted with a flame ionization detector and an HP-PLOT column. CO, CO_2, and H_2 were quantified on a Kristall 4000 chromatograph (Khromatek, Russia) fitted with a thermal conductivity detector and an SKT column. Low CO concentrations (<0.4 vol %) were measured using an RI-550A gas analyzer (RikenKeiki, Japan) with an IR cell.

The liquid organic products of the reaction in the aqueous and organic phases were identified by the GC–MS method using MSD 6973 (Agilent, United States) and Automass-150 (Delsi Nermag, France) devices equipped with HP-5MS and CPSil-5 columns. Organic compounds were quantified by gas–liquid chromatography (GLC) on a Varian 3600 chromatograph (Varian, United States) with a Khromtek SE-30 column using trifluoromethylbenzene as the internal standard. The residual concentration of organic products in the liquid phase was determined by the GC–MS method from integral signal ratios using absolute calibration.

COMPUTATIONAL DETAILS

The surface of the reduced alumina–platinum catalyst was modeled by the cluster method. Calculations were carried out within density functional theory (DFT) using PBE exchange–correlation density functional [16], the SBK basis set (with corresponding effective core potentials for the heavy atoms) [17, 18], and the PRIRODA 13 program [19, 20]. For open-shell systems, we used the unrestricted Kohn–Sham (UKS) method.

After optimization of the model cluster geometry, we optimized the structure of the pre-reaction complex and performed transition state calculations for the elementary steps of the reaction. The transition states obtained were tested for the existence of an imaginary frequency in the spectrum of harmonic vibrations of the calculated structure, and it was checked whether these transition states connect the reactants and the products along the reaction coordinate.

The values of enthalpy and Gibbs free energy were calculated for 350°C by finding the total energy due to the enthalpic contribution determined using the harmonic oscillation model. At this temperature and a total pressure no higher than a few atmospheres in the system, the reactants and reaction products are in the gaseous state (there is no need to take into account the solvent effect). The calculated values are not thermodynamically accurate, but their comparative analysis allows drawing semiquantitative conclusions as to the height of the activation barrier, thus making it possible to identify the rate-limiting step. In addition, this analysis can show whether one reaction or another is possible at a given temperature.

Table 1. Composition of the products of ethanol and ethylene conversion over the AP-64 catalyst at 350°C

Conversion products, wt %	Ethanol		Ethylene		
	reductive pre-activation time, h				
	4	12	4	8	12
CO_x	8.5	26.0	–	–	–
H_2	–	0.1	–	–	–
C_1	3.5	12.0	–	–	–
C_2	18.5	17.5	–	–	–
$C_{=2}$	59.5	–	94.0	90.0	69.6
C_3	1.5	5.5	–	0.2	0.1
C_4	8.5	11.2	6.0	1.8	8.2
C_5	–	2.1	–	0.8	2.2
C_6	–	12.7	3.0	9.0	–
C_7	–	1.3	–	0.9	2.5
C_8	–	3.6	–	1.8	5.8
C_9	–	0.6	–	0.3	0.7
C_{10}	–	1.6	–	0.8	0.8
C_{11}	–	0.2	–	0.2	0.6
C_{12}	–	0.2	–	0.2	0.5
C_{3-12}	–	39.0	–	10.0	30.4
Oxygenates	–	5.4	–	–	–

RESULTS AND DISCUSSION

The catalyst pre-activation time has a significant effect on the composition of the oxidation products at 100% ethanol conversion. With the catalyst reduced for 4 h, ethanol at 350°C and an hourly space velocity of 0.6 h^{-1} turns almost completely into carbon oxides, methane, ethane, and a butane–butylene fraction (Table 1). Ethanol dehydration over the catalyst reduced for 12 h gives a C_3–C_{12} alkane fraction, whose yield is 39.0%, and a minor amount (5%) of olefins. The specific alkane fraction production rate is 0.19 g per gram of catalyst per hour.

The addition of ethylene to ethanol in the presence of the catalyst subjected to prolonged reduction increases the proportion of hydrocarbons containing an even number of carbon atoms in the C_3–C_{12} fraction (Fig. 1). The proportion of C_8 and C_{10} hydrocarbons increases to the greatest extent (as a result of consecutive conversions of C_4 and C_6 alkanes).

The duration of the reduction of the alumina–platinum catalyst has an effect on ethylene conversion as well. In the presence of the unreduced catalyst at 350°C, ethylene is stable. Over the catalyst pre-reduced for 4 h, ethylene turns into small amounts of butanes and butylenes (2 and 4%, respectively) (Table 1). With the catalyst pre-activated by reduction for a longer time of 8 h, the ethylene conversion is 10% and a C_3–C_{12} olefin fraction dominated by hydrocarbons with an even number of carbon atoms appears in the product (Table 1). On passing to the catalyst pre-reduced for 12 h, the C_3–C_{12} hydrocarbon yield increases to 30.4% and the hydrocarbons containing an even number of carbon atoms remain dominant components of the fraction (Table 1). Hydrocarbons

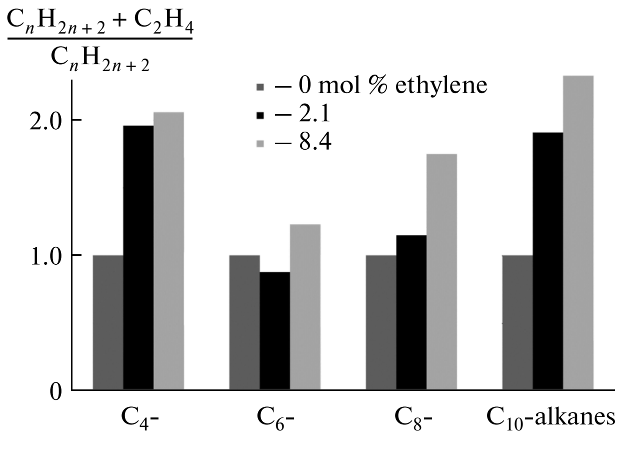

Fig. 1. Effect of ethylene added to ethanol on the relative yield of alkanes with an even number of carbon atoms.

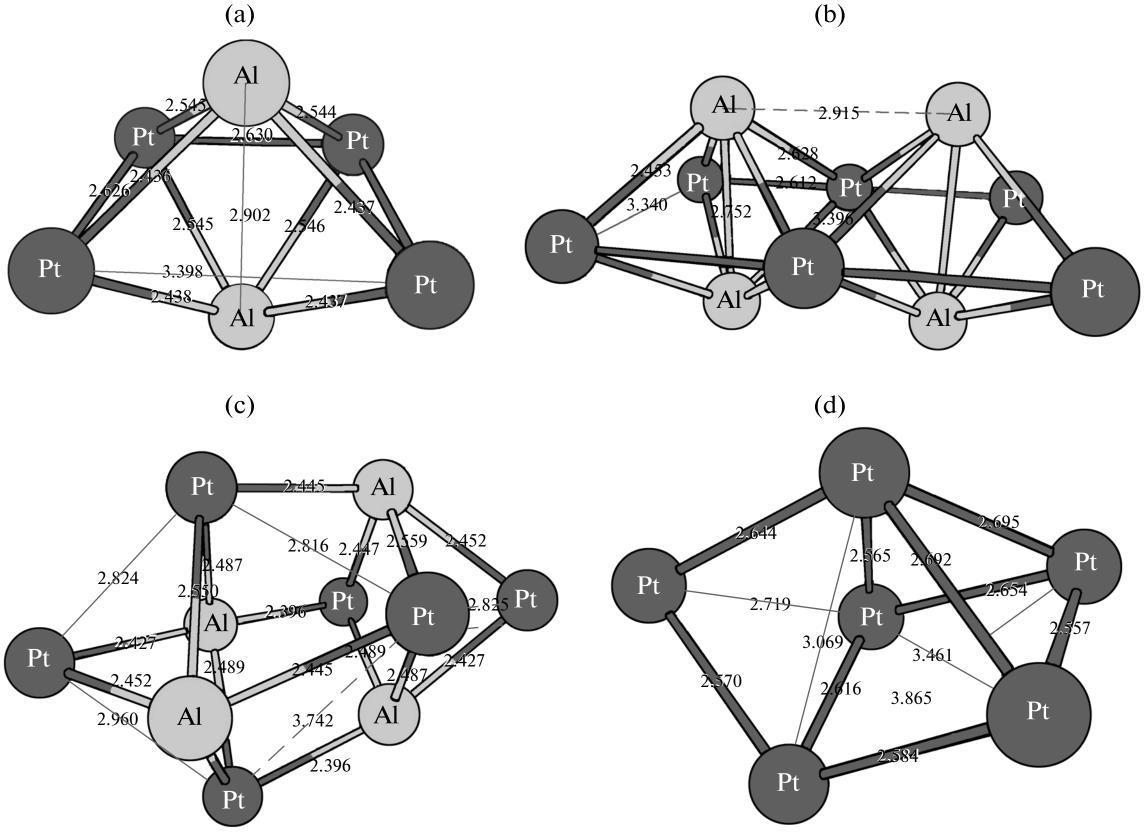
(a) (b) (c) (d)

Fig. 2. Model clusters: (a) Pt_4Al_2, (b) Pt_6Al_4 obtained by augmenting the Pt_4Al_2 cluster, (c) Pt_6Al_4 corresponding to the energy minimum, and (d) Pt_6 (for comparative calculations).

with an odd number of carbon atoms likely result from cracking reactions.

As was demonstrated in an earlier study [11], diethyl ether in the presence of the reduced catalyst turns into a mixture of hydrocarbons whose composition is similar to the composition of the ethanol conversion products. It is doubtful that diethyl ether forms on platinum–aluminum clusters. (Most likely, it forms via an additional ethylene donation pathway involving acid sites, which can participate in chain propagation).

The above results indicate that the commercial alumina–platinum catalyst changes its selectivity as a result of prolonged reductive activation. In this case, ethanol turns into an C_3–C_{12} alkane fraction, while ethylene turns into a C_3–C_{12} olefin fraction (Table 1). It was observed earlier that the hydrogen that is necessary for alkane formation results from parallel ethanol dehydrogenation reactions [11]:

$$C_2H_5OH \rightarrow CH_4 + CO + H_2,$$

$$CO + H_2O \rightarrow CO_2 + H_2,$$

$$C_2H_5OH + H_2O \rightarrow 2CO + 4H_2.$$

In the case of ethylene, there is no source of hydrogen in the system, and this leads to the formation of only higher olefins that are ethylene oligomerization products.

For considering the main ethanol conversion steps, we carried out a theoretical analysis of ethanol conversion on platinum–aluminum sites. It would be logical to consider Pt_4Al_2 (Fig. 2a) as the model cluster, but this cluster is too small for modeling the chemisorption of two ethanol molecules. For this reason, it was augmented to a Pt_6Al_4 cluster (Fig. 2b). The optimized structure of this cluster is presented in Fig. 2c. It is this structure that was used in the calculation of reaction pathways. For the sake of comparison, reaction pathways were also calculated for the Pt_6 cluster (Fig. 2d).

The geometric parameters of the clusters were optimized for different electronic states with spin multiplicities of $M = 1, 3, 5, 7, 9$, and 11. The relative values of the total energy of these clusters without and with the zero-point energy taken into account (E and E_0, respectively) are listed in Table 2. Clearly, high-spin states are energetically favorable for the Pt_6 cluster, which is in agreement with the literature [21], and low-spin states are energetically favorable for the intermetallic cluster. At the same time, the difference between the energies of a number of states is relatively small. For this reason, in these calculations both model clusters were taken to be in the triplet state.

We found a number of stationary points on the potential energy surface that correspond to the transition states of different steps and intermediates. On being adsorbed on the intermetallic cluster (Fig. 3a), the ethanol molecule loses hydrogen from its methyl group (the transition state and intermediate are shown in Figs. 3b and 3c, respectively). Next, hydrogen is transferred from one Pt atom to a position between two Pt atoms (the transition state and intermediate are shown in Figs. 3d and 3e, respectively). This is followed by hydroxyl group transfer to an Al atom, and, as a result, adsorbed ethylene coordinates to the Pt atom (the transition state and intermediate are shown in Figs. 3f and 3g, respectively). The adsorption of the second ethanol molecule takes place in the same way, but with slightly higher activation barriers. The decomposition of the second ethanol molecule on the given cluster occurs in the same way as the decomposition of the first one, with the only difference that its second step is a rotation of the hydroxyl group of ethanol rather than the shift of hydrogen from one position to another. In both cases, these steps are opposed by no barriers and exert no significant effect on the overall process.

The same calculations were carried out for the case of the hydroxyl group of ethanol coordinated to a Pt atom. A series of similar structures was obtained, but the relationship of activation barriers turned out to be somewhat different and closer to that calculated for the Pt_6 cluster. In addition, some of the steps that are observed in the above case and are characterized by an insignificant change in free energy and a negligible activation barrier are missing in this case. The calculated values of thermodynamic and activation parameters of some steps are listed in Table 3.

The hypothetical steps of the adsorption of ethanol followed by its conversion into ethylene are very likely for all of the three cases described above. In the chemisorption of the first ethanol molecule by the Pt–Al atomic pair, the rate-limiting step is C–H bond breaking, while the rate-limiting step in the chemisorption of the same molecule by the Pt–Pt atomic pair is C–O bond breaking. Moreover, the lowest activation barriers were obtained for ethanol chemisorption on the Pt_6 cluster.

The chemisorption of the second ethanol molecule on the platinum–aluminum site is possible, but it is opposed by a much higher activation barrier, while in the chemisorption on two Pt atoms (both in the intermetallide and in platinum metal), the activation barrier to the rate-limiting step remains practically unchanged.

Another significant distinction between ethanol chemisorption on two Pt atoms of the Pt_6Al_4 cluster and ethanol adsorption on the Pt–Al atomic pair is that, in the former case, one of the hydroxyl groups passes from the Pt atom to an Al atom during the breaking of the C–O bond in the second ethanol molecule. This markedly lowers the activation barrier of this step and makes this step and, in particular, the chemisorption of the ethanol molecule energetically favorable.

Table 2. Relative energies of the Pt_6Al_4 and Pt_6 clusters

*M**	Pt_6Al_4		Pt_6	
	E	E_0	*E*	E_0
	kcal/mol			
1	0	0	3.2	3.2
3	2.1	2.1	4.2	4.2
5	14.1	13.8	1.2	1.2
7	48.8	48.4	0	0
9	85.2	85.0	0.7	0.9
11	129.4	128.9	45.0	44.9

* *M* is spin multiplicity.

An analysis of the probability of ethylene dimerization occurring on Pt atoms (one of the possible variants) demonstrates that the activation barrier to this reaction (for both model clusters) is very high; that is, this reaction is unlikely. No separate calculations were performed for ethylene dimerization in the case of the initial coordination of the hydroxyl group of ethanol to a Pt atom, because this system does not differ radically from the system in which the ethanol hydroxyl is initially coordinated to an Al atom. We were unable to obtain structures corresponding to ethylene adsorption on Al atoms.

Note that, in the case of ethanol chemisorption on two Pt atoms of the Pt_6Al_4 cluster, it is very likely that the hydroxyl group will be transferred into the coordination sphere of an adjacent Al atom. (The activation barrier to this transfer is relatively low and does not depend on which of the nonequivalent Al atoms the hydroxyl is transferred.) In the case of ethanol chemisorption (Fig. 3), hydroxyl groups appear on Al atoms as well. Thus, in both cases there are favorable conditions for the formation of a strong protonic acid site, and this was indeed demonstrated experimentally [11, 22]. It can be hypothesized that these protonic acid sites, which form in the course of the reaction, are the places where the olefin chain grows [23, 24].

Ethylene must desorb from the platinum sites. Calculations demonstrated that ethylene desorption is energetically favorable (or is accompanied by a relatively small increase in free energy) primarily when the ethanol molecule is chemisorbed on platinum–aluminum sites. In case ethanol is chemisorbed on the Pt_6 cluster or at least one hydroxyl group is present on at least one Pt atom, desorption is energetically less favorable.

It follows from the above analysis that it is the platinum–aluminum sites that can be active sites in the

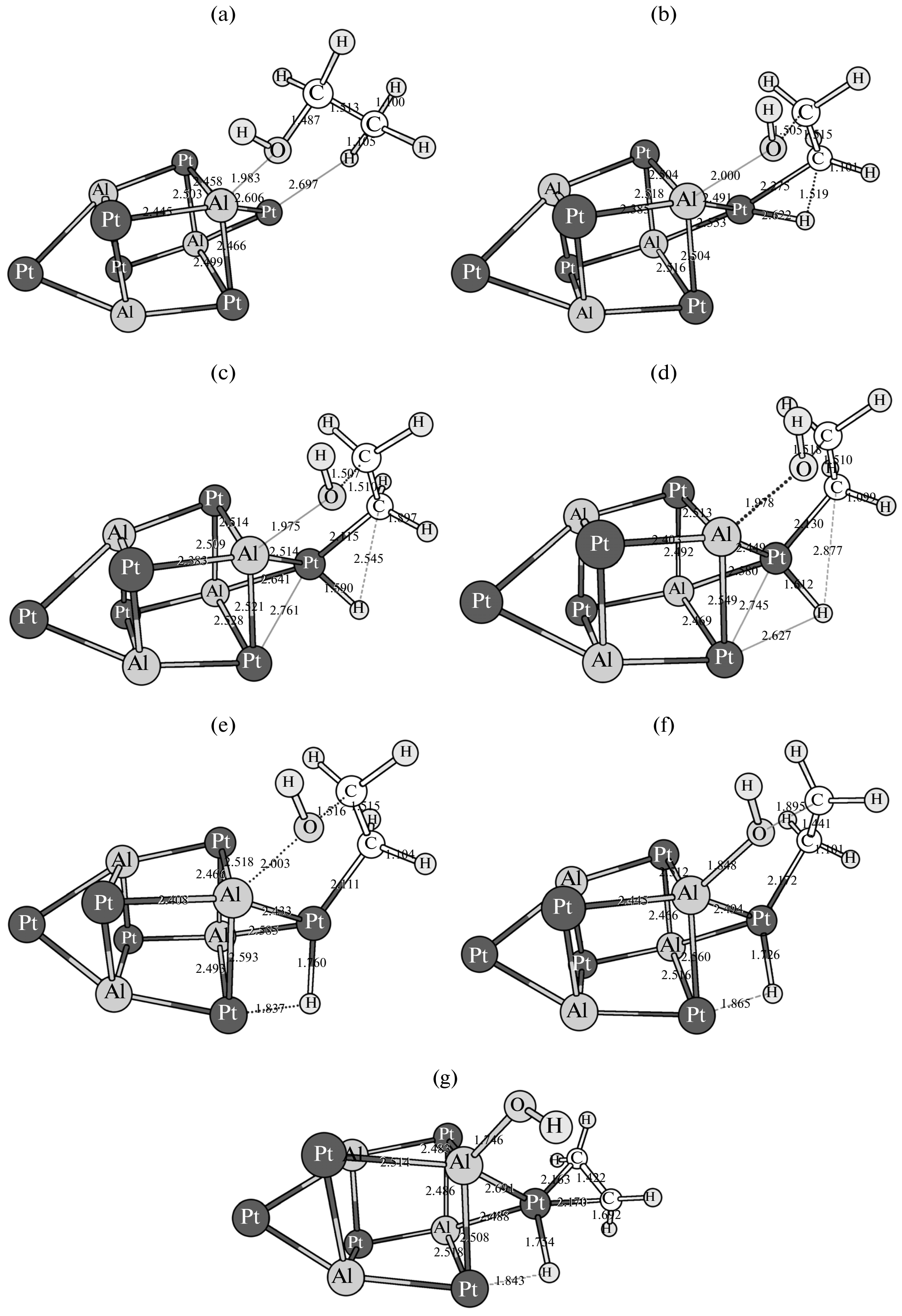

Fig. 3. Stationary points found on the potential energy surface for ethylene formation from ethanol on the Pt_6Al_4 cluster: (a) prereaction complex, (b) transition state in the breaking of the C–H bond, (c) intermediate 1, (d) transition state in the shift of the hydrogen atom, (e) intermediate 2, (f) transition state in the breaking of the C–O bond, and (g) post-reaction complex.

Table 3. Calculated energetic parameters (kcal/mol) for the basic steps of ethylene formation from ethanol and for some other reactions occurring in the system at 350°C

Elementary step	Pt_6Al_4, on Al atom				Pt_6Al_4, on Pt atom				Pt_6			
	ΔH	ΔG	ΔH_A	E_A	ΔH	ΔG	ΔH_A	E_A	ΔH	ΔG	ΔH_A	E_A
Adsorption of an EtOH molecule	–19.5	4.4	–	–	–4.8	10.2	–	–	–16.5	10.9	–	–
C–H bon breaking by a Pt atom	3.9	5.3	18.2	19.9	–3.1	5.5	10.7	19.4	–19.1	–15.9	6.3	2.3
Proton transfer between Pt atoms	–4.4	–7.0	–1.0	–2.3	–10.1	–10.1	–1.2	–0.7	–	–	–	–
C–O bond breaking	–32	–35.9	3.3	2.5	–2.9	–7.1	23.2	20.7	–16.1	–26.3	15.7	13.9
Sum total for the chemisorption of the first EtOH molecule	–52.0	–33.3	–	–	–20.9	–1.4	–	–	–51.7	–31.3	–	–
Desorption of a C_2H_4 molecule	30.7	9.3	–	–	32.2	9.9	–	–	38.0	16.2	–	–
OH group transfer	–	–	–	–	–33.6	–33.0	0.9	4.3	–	–	–	–
from Pt to Al	–	–	–	–	–32.5	–32.7	8	11.7	–	–	–	–
Adsorption of the second EtOH molecule	–16.5	3.4	–	–	–7.5	10.3	–	–	–20.2	–3.1	–	–
C–H bon breaking by a Pt atom	15.2	20.8	26.7	35.7	–9.0	–0.8	10.7	18.3	–8.5	1.7	4.1	14.3
Rotation of the OH group	–0.7	–0.6	–1.0	–1.5	–	–	–	–	–	–	–	–
C–O bond breaking	–32.0	–37.4	0.7	–1.0	–29.3	–34.5	19.5	19.1	–13.5	–19.9	18.4	15.4
Sum total for the chemisorption of the second EtOH molecule	–33.9	–13.8	–	–	–45.7	–25.0	–	–	–42.0	–20.5	–	–
Direct dimerization of C_2H_4	1.1	9.0	49.4	55.2	–	–	–	–	13	21.4	43.2	51.6
Desorption of one	26.4	2.8	–	–	27.4	5.5	–	–	39.7	15.1	–	–
C_2H_4 molecule	15.1	–7.5	–	–	25.9	5.4	–	–	31.6	9.1	–	–
Desorption of both C_2H_4 molecules	40.7	–1.9	–	–	57.3	13.5	–	–	71.5	28.3	–	–

selective formation ethylene as an intermediate product in the formation of heavier hydrocarbon fraction. The role of platinum is hydrogen transfer and C–H bond breaking, and aluminum serves to transfer the hydroxyl and to diminish the change in free energy in the desorption of the resulting ethylene.

CONCLUSIONS

The results of this study and earlier experimental data suggest that the prolonged reduction of the alumina–platinum catalyst followed by steam treatment of the catalyst generates two main factors having an effect on the selectivity of the catalyst in the reductive dehydration of ethanol, namely, strong interaction between the reduced platinum and aluminum to the extent of the formation of intermetallic clusters and the transformation of aprotic acid sites on the alumina surface into strong protonic acid sites.

It was demonstrated [26] by ^{29}Al NMR spectroscopy that Pt^{4+} ions supported on the γ-Al_2O_3 surface are selectively chemisorbed by (“stick” to) pentacoordinated Al^{3+} ions [25].

The reductive dehydration of ethanol into C_{3+} alkanes is a complicated process consisting of consecutive and parallel reactions [11]. Moreover, the mechanism of hydrocarbon chain propagation is catalyst-dependent. In the presence of zeolite-based catalytic systems, chain propagation takes place via the so-called hydrocarbon pool mechanism, which leads mainly to the formation of aromatic hydrocarbons [25, 26]. In ethanol conversion over the WO_3–Re_2O_7/Al_2O_3 catalytic system, the basic chain propagation step is aldol condensation [4, 25].

Experimental data and theoretical analysis suggest that the formation of platinum–aluminum sites is favorable for ethanol conversion into ethylene, which is held by these sites and serves as the main building block for the propagation of hydrocarbon chains containing mostly containing an even number of carbon atoms. Another function of the platinum–aluminum sites is transfer of hydrogen forming in situ as a result of dehydrogenation reactions occurring in parallel, which are described in detail in an earlier work [8]. Excess hydrogen supplied to the reaction zone hampers chain propagation by hydrogenating ethylene forming from ethanol and suppresses ethane desorption from the catalysts surface [8].

The second basic step of the process yields a C_{4+} olefin fraction as a result of ethylene oligomerization. It can be hypothesized that, in this step, ethylene diffuses (“creeps over”) to strong acid sites on which hydrocarbon chain propagation takes place. Hydrogen spillover on platinum-containing sites catalyzes olefin hydrogenation into a C_{3+} alkane fraction, which is the main product of ethanol conversion over the reduced AP-64 catalyst. A possible process yielding hydrocarbons with an odd number of carbon atoms is cracking.

The theoretical models presented in this work provide the first (simplest) approximation for the reaction sites examined and disregard the effect of the γ-Al_2O_3 support. We are going to investigate the possible reactions of ethanol and ethylene molecules on the model clusters in greater detail.

ACKNOWLEDGMENTS

This study was supported by the Russian Science Foundation, Agreement no. 15-13-30034.

REFERENCES

1. Schlaf, M., *Dalton Trans.*, 2006, p. 4645.
2. Varfolomeev, S.D., Moiseev, I.I., and Myasoedov, B.F., *Herald Russ. Acad. Sci*, 2009, vol. 79, p. 334.
3. Maher, D. and Bressler, D.C., *Bioresour. Technol.*, 2007, vol. 98, p. 2351.
4. Chistyakov, A., Tsodikov, M., Chudakova, M., Gekhman, A., Moiseev, I., and Luk, F., *Chem. Eng. Trans.*, 2011, vol. 24, p. 175.
5. Chistyakov, A., Gubanov, M., and Tsodikov, M., *Chem. Eng. Trans.*, 2013, vol. 32, p. 1093.
6. Tsodikov, M.V., Yandieva, F.A., Chistyakov, A.V., Gubanov, M.A., Gekhman, A.E., and Moiseev, I.I., *Dokl. Chem.*, 2012, vol. 447, part 2, p. 306.
7. Tsodikov, M.V., Chistyakov, A.V., Gubanov, M.A., Murzin, V.Yu., Bukina, Z.M., Kolesnichenko, N.V., and Khadzhiev, S.N., *Pet. Chem.*, 2013, vol. 53, no. 1, p. 46.
8. Yandieva, F.A., Kugel, V.Y., Chistyakov, A.V., Gekhman, A.E., and Moiseev, I.I., *Catal. Lett.*, 2008, vol. 121, p. 199.
9. Tsodikov, M.V., Chistyakov, A.V., Yandieva, F.A., Zhmakin, V.V., Gekhman, A.E., and Moiseev, I.I., *Catal. Ind.*, 2011, vol. 3, no. 1, p. 4.
10. Yandieva, F.A., Tsodikov, M.V., Gekhman, A.E., and Moiseev, I.I., *Russ. Chem. Bull.*, 2012, vol. 61, no. 8, p. 1669.
11. Yandieva, F.A., Tsodikov, M.V., Chistyakov, A.V., Kugel’, V.Ya., Zubavichus, Ya.V., Veligzhanin, A.A., Kitaev, L.E., Yushchenko, V.V., Gekhman, A.E., and Moiseev, I.I., *Kinet. Catal.*, 2010, vol. 51, no. 4, p. 548.
12. Liberman, A.L., Bragin, O.V., and Vasina, T.V., *Bull. Acad. Sci. USSR, Div. Chem. Sci.*, 1964, vol. 13, no. 7, p. 1266.
13. Tsodikov M.V., Chistyakov A.V., Gubanov M.A., Khadzhiev S.N., Gekhman A.E., and Moiseev I.I. *Russ. Chem. Bull.*, 2013, vol. 62, no. 3, p. 820.
14. Chistyakov, A.V., Tsodikov, M.V., Murzin, V.Yu., Yandieva, F.A., Zubavichus, Ya.V., Kozitsyna, N.Yu., Gekhman, A.E., Kriventsov, V.V., and Moiseev, I.I., *Kinet. Catal.*, 2011, vol. 52, no. 2, p. 258.
15. Tsodikov, M., Murzin, V., Chistyakov, A., Yandieva, F., Gubanov, M., Zharova, P., Shapovalov, S., Tikhonova, O.,

and Pasynskii, A., *Chem. Eng. Trans.*, 2014, vol. 37, p. 583.

16. Perdew, J.P., Burke, K., and Ernzerhof, M., *Phys. Rev. Lett.*, 1996, vol. 77, no. 18, p. 3865.
17. Stevens, W.J., Basch, H., and Krauss, M., *J. Chem. Phys.,* 1984, vol. 81, no. 12, p. 6026.
18. Stevens, W.J., Krauss, M., Basch, H., and Jasien, P.G., *Can. J. Chem.*, 1992, vol. 70, p. 612.
19. Laikov, D.N., *Chem. Phys. Lett.*, 1997, vol. 281, p. 151.
20. Laikov, D.N. and Ustynyuk, Yu.A., *Russ. Chem. Bull.*, 2005, vol. 54, no. 3, p. 820.
21. Sebetci, A., *Phys. Chem. Chem. Phys.*, 2011, vol. 11, p. 921.
22. Yushchenko, V.V. and Romanovskii, B.V., *Russ. J. Phys. Chem. A*, 1997, vol. 71, no. 11, p. 1852.
23. Grigor’eva, N.G., Bubennov, S.V., and Kutepov, B.I., *Catal. Ind.*, 2011, vol. 3, no. 2, p. 144.
24. Grigor’eva, N.G., Talipova, R.R., Khazipova, A.N., Bubennov, S.V., Kutepov, B.I., and Dzhemilev, U.M., *Pet. Chem.*, 2009, vol. 49, no. 1, p. 16.
25. Zharova, P.A., Chistyakov, A.V., Zavelev, D.E., Kriventsov, V.V., Yakimchuk, E.P., Kryzhovets, O.S., Petrakova, O.V., Drobot, D.V., and Tsodikov, M.V., *Russ. Chem. Bull.,* 2015, vol. 64, no. 2, p. 337.
26. Hu, J., Mei, D., Yi, C.-W., Kim, D.H., Peden, C.H.F., Allard, L.F., and Szanyi, J., *Science*, 2009, vol. 325, p. 1670.

Translated by D. Zvukov